AD-A115 243 AIR FORCE GEOPHYSICS LAB HANSCOM AFB MA F/G 4/2
IONOSPHERIC MODELING.(U)
JAN 82 B S DANDEKAR
UNCLASSIFIED AFGL-TR-82-0024 NL

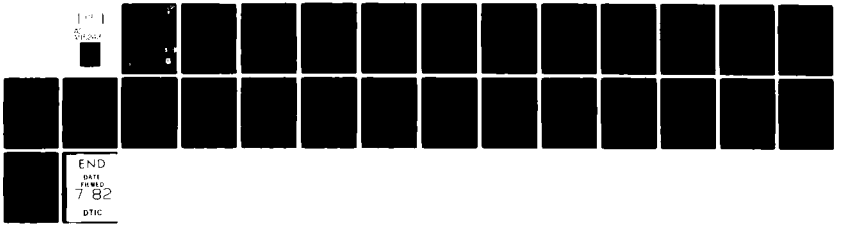

END
DATE FILMED
7 82
DTIC

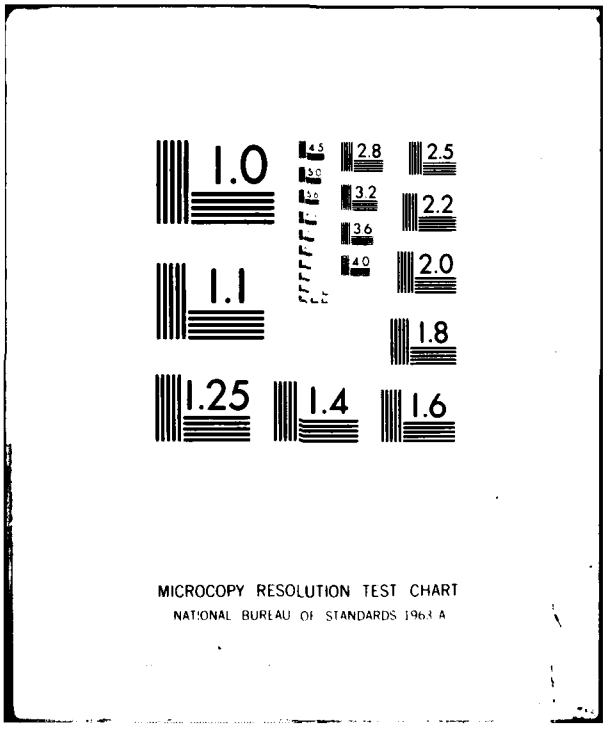
1.0
1.1
1.25
1.4
1.6
1.8
2.0
2.2
2.5
2.8
3.2
3.6
4.0
4.5
5.0
5.6
6.3
7.1
MICROCOPY RESOLUTION TEST CHART
NATIONAL BUREAU OF STANDARDS 1963 A

AD A115243

AFGL-TR-82-0024
ENVIRONMENTAL RESEARCH PAPERS, NO. 788

Ionospheric Modeling

B. S. DANDEKAR

27 January 1982

Approved for public release; distribution unlimited

DTIC
ELECTE
S
D

SPACE PHYSICS DIVISION PROJECT 4643
AIR FORCE GEOPHYSICS LABORATORY
HANSCOM AFB, MASSACHUSETTS 01731

AIR FORCE SYSTEMS COMMAND, USAF

DTIC FILE COPY

82 04 07 [illegible]

This report has been reviewed by the ESD Public Affairs Office (PA) and is releasable to the National Technical Information Service (NTIS).

This technical report has been reviewed and is approved for publication.

Alva T. Stair, Jr.

DR. ALVA T. STAIR, Jr
Chief Scientist

Qualified requestors may obtain additional copies from the Defense Technical Information Center. All others should apply to the National Technical Information Service.

Unclassified

SECURITY CLASSIFICATION OF THIS PAGE (When Data Entered)

REPORT DOCUMENTATION PAGE		READ INSTRUCTIONS BEFORE COMPLETING FORM
1. REPORT NUMBER AFGL-TR-82-0024	2. GOVT ACCESSION NO. AD-A115243	3. RECIPIENT'S CATALOG NUMBER
4. TITLE (and Subtitle) IONOSPHERIC MODELING		5. TYPE OF REPORT & PERIOD COVERED Scientific. Final. 6. PERFORMING ORG. REPORT NUMBER ERP No. 768
7. AUTHOR(s) B. S. Dandekar		8. CONTRACT OR GRANT NUMBER(s)
9. PERFORMING ORGANIZATION NAME AND ADDRESS Air Force Geophysics Laboratory (PHY) Hanscom AFB Massachusetts 01731		10. PROGRAM ELEMENT, PROJECT, TASK AREA & WORK UNIT NUMBERS 62101F 46430609
11. CONTROLLING OFFICE NAME AND ADDRESS Air Force Geophysics Laboratory (PHY) Hanscom AFB Massachusetts 01731		12. REPORT DATE 27 January 1982 13. NUMBER OF PAGES 27
14. MONITORING AGENCY NAME & ADDRESS(if different from Controlling Office)		15. SECURITY CLASS. (of this report) Unclassified 15a. DECLASSIFICATION DOWNGRADING SCHEDULE

16. DISTRIBUTION STATEMENT (of this Report)

Approved for public release; distribution unlimited.

17. DISTRIBUTION STATEMENT (of the abstract entered in Block 20, if different from Report)

18. SUPPLEMENTARY NOTES

19. KEY WORDS (Continue on reverse side if necessary and identify by block number)

Ionosphere
Ionospheric models
Ionospheric predictions

20. ABSTRACT (Continue on reverse side if necessary and identify by block number)

The purpose of this report is to familiarize a user of ionospheric models with the options presently available for ionospheric prediction and specification. Two types of ionospheric models are available: the numerical-phenomenological and theoretical models. From the numerical type, the ITS-78, IONCAP, and Bent models have been discussed. In the theoretical models the main concern is the number of parameters included in the model. Nine ionospheric models available have been summarized. The differences and limitations of these models are compared and tabulated. This information

DD FORM 1 JAN 73 1473

Unclassified

SECURITY CLASSIFICATION OF THIS PAGE (When Data Entered)

20. (Cont)

will help a user make a judicious selection of an ionospheric model to satisfy his specific needs. The sources for obtaining the programs for these models have been listed for ready reference.

Preface

The author thanks Drs. Jules Aarons and Jurgen Buchau for many useful comments and their interest in the work.

Accession For
NTIS GRA&I ☒
DTIC TAB ☐
Unannounced ☐
Justification
By
Distribution/
Availability Codes
Dist | Avail and/or Special
A

DTIC COPY INSPECTED 2

Contents

Illustrations

PRECEDING PAGE BLANK-NOT FILMED

Tables

Ionospheric Modeling

1. INTRODUCTION

The reflection, transmission, refraction, and scattering characteristics of the ionosphere have been used for radio communication since the discovery of the ionosphere in the earth's atmosphere. For successful radio communication, it is essential to predict the behavior of the ionospheric region that will affect a given radio communication circuit. Such a prediction will identify the time periods, the path regions and the sections of high frequency bands which will allow or disrupt the use of the selected high frequency communication circuit. This need for prediction leads to modeling of the ionosphere.

A model is a numerical statistical description of the ionosphere in terms of location (geographic or geomagnetic latitudes and longitudes, time (solar zenith angle), seasons, and other factors such as the solar activity (10.7 cm flux, sunspot numbers). The empirical equations are derived from the dependence of the observed phenomena on various parameters mentioned above. These observed phenomena include: the behavior of critical frequencies* foE, foF_1, foF_2, and foEs for the E, F_1, F_2, and sporadic E layers; the altitudes for peak (maximum) electron densities

(Received for publication 26 January 1982)

*The critical frequency is the limiting radio frequency below which a radio wave is reflected by, and above which it penetrates and passes through, the ionized medium (an ionospheric layer) at vertical incidence.

for the layers h_mE, h_mF_1, and h_mF_2 and the half-thickness widths** y_mE, y_mF_1; and y_mF_2. These models are called phenomenological models.[1-5]

The ITS-78[1] model, based on the analysis by Jones et al[6] of world-wide, ground-based ionosonde data, predicts only the bottomside of the ionosphere. The Bent model[2] predicts the total electron content of the ionosphere in the altitude range from 150 to 2000 km, without a direct consideration of the bottomside E and F_1 layers. The Ching and Chiu model[3] covers the altitude range from 110 to 1000 km. Instead of parabolic layers[1] they assume Chapman functions for the electron density distributions in the E, F_1, and F_2 layers. Later Chiu[4] modified the Ching-Chiu model[3] to incorporate the polar ionosphere. Their models are useful only for studying the large scale phenomena such as global thermospheric and ionospheric calculations.

Using ionospheric data from ESRO satellites, Kohnlein[5] extended the altitude range up to 3500 km. He suggested a "differential approach" for the ionospheric modeling. He separated small scale special structures such as the equatorial trough, the mid-latitude trough and the polar ionosphere, from the large scale global structure. He modeled these individual structures and added them into the global structure. His method reduces the number of coefficients otherwise needed to model the complicated ionospheric behavior.

The other approach for ionospheric predictions is to use theoretical models.[8-12] These are based on the physical processes responsible for the production, maintenance and decay of the ionosphere. A theoretical model would thus rely on the process of ionization of neutral atmospheric constituents by the incident solar extreme ultraviolet radiation, the transport processes such as diffusion and neutral winds, and also on the effect of electric and magnetic fields on the transport processes. Essentially the theoretical model tries to explain the experimental observations in terms of known physical processes. In addition, this approach seeks new physical processes to explain the differences between the observational results and the predictions based on the theoretical considerations.

Radio communication can be divided in two main categories. Ground-to-ground radio communication is based on the reflection and scattering characteristics of the ionospheric layers. On the other hand, ground to satellite, satellite to ground, or satellite to satellite radio communications rely on the transmission and refraction characteristics of the ionosphere. The main goal of any modeling effort is to predict the periods of good or poor radio communications for the selected paths to enable a continuous undisrupted communication through the ionosphere or by some other means.

** The half-thickness width y_m of the ionospheric layer is determined with the assumption that the layer has a parabolic shape.[7]

(Due to the large number of references cited above, they will not be listed here. See References, page 25.)

In the following we will consider several ionospheric models which are routinely used (or are available) for the prediction and specification of the ionosphere. The emphasis here is on acquainting the user with the modeling programs and their limitations. This report in no way attempts to review the scientific literature for a determination of the state of the art of modeling efforts. Therefore only the essential references will be cited in the following text.

First, we will consider the numerical-phenomenological models. Then we will consider the theoretical models. This will be followed by the modifications to models to take into account high latitude phenomena such as the auroral E layer and the mid-latitude F region trough. In the conclusion section, we will look at the limitations of these models and a possible approach to overcome these limitations.

2. THE NUMERICAL-PHENOMENOLOGICAL MODELS

At present the three most widely used numerical models for ionospheric predictions are: (1) The ITS-78 model, (2) The Bent model, and (3) The Ionospheric Communications Analysis and Prediction Program (IONCAP). In addition, the 4-D model of the Air Force Global Weather Central and the Bradley model will be considered.

2.1 The ITS-78 Model

The main purpose of this model[1] is to predict long term performance of communication systems operating in the 2-30 MHz frequency range. The model serves an essential function of assistance in the planning, design, and operation of high frequency (HF) communication systems.

The model provides (output) circuit operational parameters such as the maximum usable frequency (MUF), optimum traffic frequency (FOT), and the lowest usable frequency (LUF). In addition to the regular E-layer propagation mode, it takes into account propagation via the sporadic E layer. The program computes all the probable modes. It computes the system performance. For that purpose it calculates the antenna patterns and gains for 10 most commonly used antennas. It also has a program to determine MUF as a function of the magnetic activity index Kp.

The inputs for the ITS-78 model are the date, Universal Time, geographical location (latitude and longitude) of the transmitter and receiver, and sunspot number. To compute the system performance the model needs the antenna parameters, the radiation power of the transmitter, and the signal to noise ratio of the receiver.

The ITS-78 model and its computer program was developed by the Institute of Telecommunication Sciences, ESSA, Boulder, Colorado. The model is based on

the presentation of the ionospheric characteristics in a form of synoptic numerical coefficients developed by Jones and Gallet[13] and improved by Jones et al.[6] The important features of the ITS-78 model are the parameters for the D, E, E_s (sporadic), and F_2 layers of the ionosphere.

For the D region the model considers only the absorption losses. The non-deviative absorption is in the form of a semi-empirical expression. It enables the user to compute the losses for the HF frequencies penetrating the D layer. The deviative absorption losses are included in the loss calculations as uncertainty factors.

For the E region the model computes the parameter foE. It assumes a constant height of 110 km for the maximum (peak) electron density of the E layer, with a constant semi-thickness of 20 km. The numerical coefficients for foE are based on the experimental ground ionosonde data during high solar activity phase in 1958, and the low solar activity phase in 1964.

For the F_2 region the model computes the parameters foF_2, the height of maximum electron density h_mF_2 and the semi-thickness y_mF_2 of the F layer. These are in the form of numerical coefficients for the high (1958) and low (1964) phases of solar activity. Both the E and F_2 layers are assumed to be parabolic in shape.

The sporadic E (E_s) layer could be very helpful or harmful to radio communications depending on the nature of the E_s layer. A blanketing, totally reflecting E_s layer extends the frequency range of the E-mode communications. However a semi-transparent or partly reflecting E_s layer would cause serious multipath and mode interference and would be detrimental to communication systems. Using numerical coefficients, the ITS-78 model computes foE_s only for the ordinary ray. (The earth's magnetic field splits the incident ray into the ordinary and the extraordinary rays.) The numerical coefficients are for both the high (1958) and low (1964) phases of solar activity. As the model does not predict the occurrence of E_s, the foE_s maps are used only when propagation via regular E layer is not possible. To compute the system performance the model incorporates three kinds of noise: galactic, atmospheric, and man-made.

To determine the operational parameters such as the maximum usable frequency (MUF), the model computes the path geometry (between the transmitter and the receiver). The parameters computed in the path geometry are the path length, path bearing (azimuth), and the solar zenith angle χ of the sun. The model computes paths for reflections from the E, E_s, and F_2 layers. These are called the E, E_s, and F_2 modes. The paths could involve one layer (single mode) and one reflection (one hop), or would involve more layers (multiple modes) and more reflections (multihop).

---

13. Jones, W. B., and Gallet, R. M. (1960) Ionospheric mapping by numerical methods, TTU Telecomm. J., 12:260.

For considering the wave propagation the electron density distribution with altitude is needed. Both the E and F layers are assumed to have parabolic shapes. The maximum usable frequency (MUF) is obtained by multiplying the critical frequency of the layer by the MUF factor M(3000). The term in parentheses refers to the standard ground distance of 3000 km between the (hypothetical) transmitter and the receiver. The experimental data for the numerical factor M(3000) (in terms of coefficients) come from 13 ionosonde stations covering the geomagnetic latitude range from 71° S to 88° N.

The stability and predictability of the E layer results in a 99 percent probability (highest) of supporting radio propagation and communication via the E layer. The next highest probability is via the regular F layer. When none of the above modes are possible, the E_s mode is considered for communication.

For computing the system performance the program allows a selection from 10 antenna patterns. The program takes into account the ground losses, ionospheric losses, free space losses, and the excess losses. The program computes the radio communication circuit reliability, service reliability, and the multipath evaluations.

The ITS-78 model has several limitations. The results from the model are useful only when the operating frequency is below the maximum usable frequency. The model assumes that transmission will be by reflection from the ionosphere. For this the transmitter and the receiver must be on the same side of the ionospheric layer (for example, ground-to-ground communication). The results cannot be applied to satellite-to-ground communications. The model does not take into account the daytime F_1 layer which usually develops between the E and F_2 layers. The model does not adequately account for the electron density above the altitude of h_mF_2. Finally, the model does not take into account the dependence of absorption on the operating frequency in considering the D-layer absorption.

2.2 The Bent Model

The Bent Model[2, 14] is basically for ground-to-satellite communication but can be adapted for ground-to-ground or satellite-to-satellite communication. The main purpose of the Bent model is to determine the total electron content (TEC) of the ionosphere as accurately as possible in order to obtain high precision values of the delay and directional changes of a wave due to refraction. Ground-to-satellite communication demands operating frequencies which are higher than the MUF. Thus the mode involves the transmission refraction characteristics of the F_2 layer and the electron density distribution above the height of the F_2 peak must be known.

---

14. Llewellyn, S.K., and Bent, R.B. (1973) Documentation and Description of the Bent Ionospheric Model, AFCRL-TR-73-0657, AD 772733.

The model provides (output) the vertical total electron content above the transmitter, the profile of vertical electron density with altitude, and the total electron content along the path between the satellite and the ground. It also provides the refraction corrections to the elevation angle, the range, and the range rate.

The input parameters to the model are the date, Universal Time, locations of the transmitter and receiver (ground and satellite), rate of change in elevation and altitude of the satellite, operating frequency, the solar flux (10.7 cm flux), and sunspot number.

The data base of the Bent model consists of 50,000 topside ionospheric soundings, 6000 satellite measurements of electron density and 400,000 bottomside soundings of the ionosphere. The data extend from 1962 to 1969 to cover the maximum and the minimum of the solar cycle.

The bottomside data are foF_2 hourly values from 14 stations in the American sector covering geographic latitudes 76° N to 12° S or geomagnetic latitudes from 85° to 0°. The topside soundings cover the period 1962 to 1966, with geomagnetic latitude range 85° to -75°, and the electron density profiles are from 1000 km down to the altitudes of the foF_2 peak (h_mF_2). The satellite data are from the Ariel 3 satellite covering the period May 1967 to April 1968 and are linked with real time foF_2 from 13 ground stations. Thus the data base of the Bent model refers to solar cycle 20, while the data base of the ITS-78 model is from solar cycle 19.

The Bent model uses foF_2 from the ITS-78 model. Instead of the monthly median values, the Bent model computes average values for every 10-day interval of the month from the 10.7 cm solar flux input. For the height h_mF_2, it uses M(3000) factors of NOAA (ITS-78) in terms of the sunspot number. It uses an empirical polynominal for M in computing h_mF_2, in place of the Shimazaki equation[15] used by ITS-78.

The distribution of electron density with altitude, assumed by the Bent model for the computation of the total electron density is shown schematically in Figure 1. Starting from the bottom, it divides the profile into five sections; a bottom biparabolic F2 layer; a parabolic F2 layer above the peak; and three exponential sections to cover the altitude above h_o (h_mF_2 to 1000 km). The construction of the profile needs the parameters k_1, k_2, k_3, Y_t, Y_m, foF_2, and h_mF_2. The last two have already been explained. The dependence of the other parameters on geomagnetic latitude, solar flux, foF_2, and the season is from work of Bent[14]. The topside and the first adjoining exponential section are matched at a height d (above h_m) by the equation

15. Shimazaki, T. (1955) World wide variations in the height of the maximum electron density of the ionospheric F_2 layer, J. Radio Res. Labs., Japan 2:86.

$$d = h_0 - h_m = \frac{1}{k_1} \left[\sqrt{1 + Y_t^2 k_1^3} - 1 \right]$$

where Y_t is the half thickness of the F_2 layer and k_1 is the exponential constant.

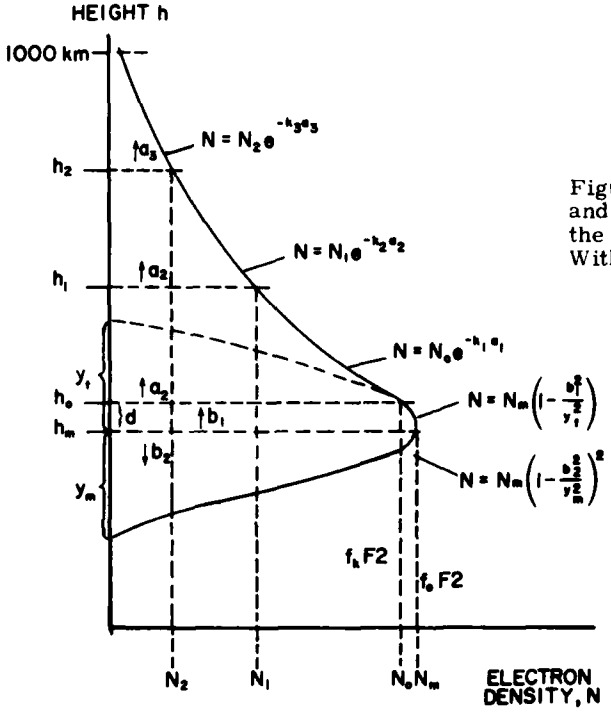

Figure 1. Schematic for Exponential and Bi-parabolic Profiles for the Electron Density Distribution With Altitude for the Bent Model

The remaining profile above the F_2 peak [of altitude range (h_m + d to 1012) km] is divided in three equal intervals of altitude.

The model can predict with an accuracy of 75 - 80 percent. If the model is updated with observed recent data within a range of 2000 km radius (from the transmitters), the predictability is improved to 90 percent.

Though the model predicts total electron content (TEC) with good accuracy, the model does not have separate E and F_1 layers. As the model was constructed for the TEC, the E and F_1 layers are included as the bi-parabolic bottomside of the F_2 layer. Also, the program does not take into account the non-deviative absorption in the underlying D layer.

2.3 The Ionospheric Communications Analysis and Prediction Program (IONCAP)

The IONCAP[16] is essentially the latest, improved, and more versatile and flexible version of the ITS-78 model.

It provides 30 output options which can be divided into four categories, (1) ionospheric description, (2) antenna patterns, (3) MUF predictions, and (4) system performance predictions.

For ionospheric predictions it provides monthly median values for the parameters foE, foF_1, foF_2, h_mE, h_mF_1, h_mF_2, Y_mE, Y_mF_1, and Y_mF_2. It also provides the lower, median, and upper decile values of the minimum of foE or foE_s. It can also provide a prediction in the form a plot of operating frequency with virtual height and also with true height.

The MUF option of the output provides the minimum radiation angle and the M factors for all four modes, E, F_1, F_2, and E_s. The plots for the diurnal variation of the MUFs are also available. The MUFs provide the description of the state of the ionosphere and do not include any system parameters. The operating frequency for a given radio communication circuit is the critical frequency of the layer multiplied by the MUF factor.

In the system performance options, 22 performance parameters are available. The program for the antenna output option computes the elevation angles and the operating frequencies for optimum view of the antenna geometry and its gain.

The input for the program is the date, Universal Time, geographical locations of the transmitter and the receiver, and sunspot number. The program can accept external ionospheric parameters as input to the program. For antenna pattern one can select the antennas from 11 antennas in the program. Antennas from ITS-78 have been modified. For the system performance additional inputs such as radiation power at the transmitter, and the S/N ratio of the receiver are needed.

The electron density distribution with altitude for the IONCAP program is shown in Figure 2. The model has 4 parabolic layers, E, F_1, and F_2. The altitudes for the peak electron densities are h_mE, h_mF_1, and h_mF_2. The half thickness widths for the layers are Y_mE, Y_mF_1, and Y_mF_2 respectively. For the F_1 layer, h_mF_1, Y_mF_1 is assumed to be 4. The E layer has fixed altitudes h_mE = 110 km and Y_mE = 20 km. IONCAP improves on the ITS-78 model by incorporating D and F_1 layers. The D layer contribution is considered indirectly by adding an exponential tail for the E layer down to the altitude of 70 km. In the transition region between the E and F_1 or F_2 if F_1 is absent) layers, the electron

---

16. Lloyd, J.L., Haydon, G.W., Lucas, D.L., and Peters, L.R. (1978) Estimating the Performance of Telecommunication Systems Using the Ionospheric Transmission Channel, National Telecommunications and Information Administration, Boulder, Colorado.

density is assumed to be linear for the frequency range f_v to f_u where $f_v = x_v \cdot foE$ and $f_u = x_u \cdot foE$. Typical values for x_v and x_u are 0.85 and 0.98 respectively. Thus the electron density decreases above the parabolic nose 0.85 foE (< foE) and continues upwards up to 0.98 foE (<foE) producing a valley in the transition region. When the $x_u = x_v = 1$ the valley is absent in the transition region and the curve is a vertical line starting at the tip of the parabolic nose of the E layer. The F_1 layer forms a linear or parabolic ledge depending on the magnitudes of h_mF_1, h_mF_2, foF_1, and foF_2. In the ITS-78 model, the F_1 layer is assumed to be absent. In the IONCAP model the numerical coefficients for foE are functions of geographic latitude for both solar maximum and minimum from the work of Leftin.[17] The model uses foF_1 maps of Rosich and Jones.[18] It also takes into account the retardation below the F_2 layer.

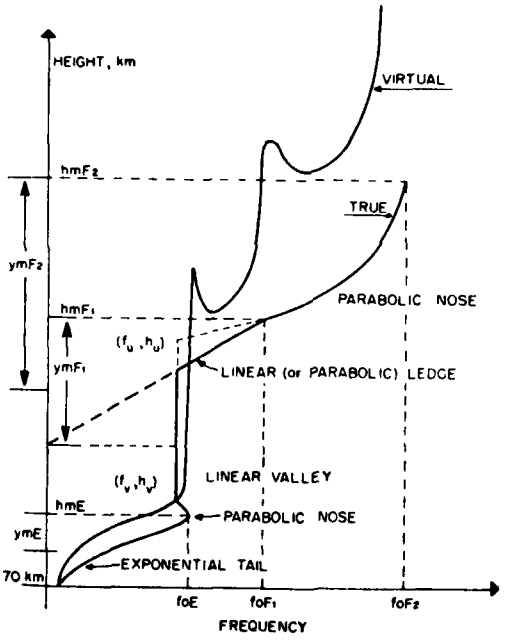

Figure 2. Schematic for the Electron Density Profile and Virtual Height for the IONCAP Model

For the MUF computations the model uses the corrected form of Martyn's theorem. As the absorption equations using the secant law do not work for lower

17. Leftin, M. (1976) Numerical Representation of Monthly Median Critical Frequencies of the Regular E. Region (F_oE), OT Report 76-88, Boulder, Colorado.

18. Rosich, R.K., and Jones W.B. (1973) The Numerical Representation of the Critical Frequency of the F_1 Region of the Ionosphere, OT Report 73-22, Boulder, Colorado.

frequencies at altitudes below 90 km, these equations have been modified in the IONCAP program. The IONCAP provides two programs (1) the ITS-78 short path geometry and (2) the long path (> 10,000 km) geometry. In addition to the ITS-78 model, the path computations now include the F_1 mode, the over-the-MUF mode, D and E region absorption losses, and sporadic E losses. A correction to frequency dependence is added for low frequencies reflected from altitudes below < 90 km.

The improvements over ITS-78 can be summarized (see IONCAP) as follows:

(1) The description of the ionosphere is now more complete.

(2) The loss equations have been supplemented. This includes E mode adjustments, sporadic E effects, over-the-MUF losses, and losses for low reflection heights.

(3) Revision is made to the ray path geometry calculations. This was an empirical adjustment to Martyn's theorem.

(4) Revision of the loss statistics was made to include the effects of the sporadic E layer and of over-the-MUF modes.

(5) A separate long path model is developed.

(6) Revisions were made to the antenna gain package.

All the models predict only the quiet ionosphere, which shows a large systematic dependence on latitude, longitude, season, time, and sunspot activity.

2.4 The Bradley Model

The Bradley model contains two modifications to the existing models: (1) the filling of the valley between the E and F layers (F_1, or F_2 if F_1 is absent), by parabolic layers,[19] and (2) a simple formulation of the prediction of the probability of the high-frequency propagation.[20]

The assumption that the electron density distribution in the E and F layers is parabolic in shape, results in a valley—a reduction in electron density between the two peak values, N_mE and N_mF—at altitudes h_mE and h_mF, respectively. The rocket observations have shown that in reality the electron density at any altitude between the altitudes h_mE and h_mF is rarely smaller than the peak electron density N_mE. Thus the assumption of the parabolic shapes for E and F layers underestimates the electron density in the altitude region between h_mE and h_mF. To correct such an underestimation Bradley and Dudeney[19] suggested a linear distribution of

19. Bradley, P.A., and Dudeney, J. R. (1973) A simple model of the vertical distribution of electron concentration in the ionosphere, J. Atmos. Terr. Phys. 35:2131.

20. Bradley, P.A., and Bedford, C. (1976) Prediction of HF circuit availability, Electronics Letters 12:32.

electron density from foE to 1.7 foE. The lower end is at $h_m E$. At the upper end, the F layer is parabolic in shape down the altitude where the plasma frequency is 1.7 foE. This linear interpolation has not yet been incorporated in the IONCAP model (see Figure 2) of Lloyd et al.[16]

In high frequency prediction it is essential to know the probability of communication at any particular operating frequency f. For convenience the observed data are expressed as F_u—the upper decile, f_m 50 percent, and F_ℓ—the lower decile of the ratios of f/f_m. The distribution functions of F_u and F_ℓ are not simple Gaussian distributions (F_u - MUF = MUF - F_ℓ for Gaussian). The distributions are χ^2-distributions of F_u and F_ℓ. For probability determinations these two χ^2-distributions (of F_u and F_ℓ) have to be used. Two variables F_u and F_ℓ with their associated degrees of freedom, and the need to integrate the χ^2-distribution curve makes the process of determining the probability distribution very cumbersome. Bradley and Bedford[20] derived simple empirical equations for this probability distribution. The equations are:

$$Q = 130 - \frac{80}{1 - \frac{1 - (f/f_m)}{1 - F_\ell}} \qquad \text{or 100, whichever is smaller for } f \le f_m$$

and

$$Q = \frac{80}{1 - \frac{(f/f_m) - 1}{F_u - 1}} - 30 \qquad \text{or 0, whichever is larger for } f > f_m ,$$

where

- Q - is the cumulative probability,
- f - is the operating frequency,
- f_m - is the predicted median frequency,
- F_ℓ - is the lower decile (of f/f_m),
- F_u - is the upper decile (of f/f_m).

They note that the probability distribution from their simple empirical equation is as good as, though not always better than, that from the χ^2 distribution. Therefore they highly recommend a replacement of χ^2 distribution procedure by these equations for a determination of the present probability that signals will propagate at a given hour over a given sky-wave path.

The latest computer model like the 'IONCAP' has not incorporated 'Bradley Features' in its program.[16]

2.5 The Air Force Global Weather Central 4-D Model

The input data to the 4-D numerical model[21] are the critical frequencies for the layers and M(3000), real time or near real time observations from 40 ground stations around the world, and total electron content (TEC) from eleven stations. The frequency of observations varies from hourly (best) at one end to weekly (worst) at the other end. The desired purpose of the 4-D model is to produce a consistent ionospheric specification anywhere in the northern hemisphere for a 24-hr period. In that sense it is not a forecasting model like the other models mentioned above.

This model has three ionospheric layers, E, F_1, and F_2. Each layer is represented by a Chapman distribution function

$$N_e(h) = N_{emax} \exp \left\{ a[1 - z - \exp(-z)] \right\}$$

where a refers to the loss mechanism and z is given by $z = \frac{h - h_{max}}{h_s}$ and h_s is the scale height for the layer. At a given altitude the total contribution to electron density is the sum of contributions by all the three layers.

For any height the electron density is approximated by

$$N_e(\ell) = \sum_{k=1}^{N} a_k W_k(\ell)$$

where a is the weighting factor and $W(\ell)$ is an empirically derived set of discrete orthogonal functions for the altitude interval 'ℓ'. The 95 to 2000 km range is divided into 127 intervals. The widths of the intervals range from 5 km at the lowest altitudes to 50 km at highest altitudes. The empirically derived function $W(\ell)$ is in two parts, spherical harmonic functions for spatial dependence and trigonometric functions (sine, cosine) for temporal dependence.

With the help of these variables a_k and W_k, the entire data base for the ionosphere is reduced to a limited number of coefficients. These can be used to construct the electron density profile, for any location in the Northern Hemisphere, valid for a 24-hr specification period. The model is still being developed. The specification accuracy of the model will strongly depend on the frequency and reliability of the input data—real-time experimental observations from the 40 ground stations of the

21. Flattery, T.W., Tascione, T.F., Secan, J.A., and Taylor, Jr., J.W. A Four-Dimensional Ionospheric Model (private communication).

northern hemisphere. Also the quality of specifications interpolated for locations inside the network will be better than those extrapolated outside the observational network.

3. THE THEORETICAL MODELS

The theoretical models for the ionosphere are based on the physical processes responsible for the observed ionospheric phenomena. The processes responsible for the ionosphere are production, maintenance, and decay of the ionosphere. As the approach deals directly with the physical processes, and not with the observed phenomena, the emerging model is called a physical model.

Four models are summarized in Table 1 to show several variations in the same processes considered by different workers. Strobel and McElroy[9] considered only the F_2 region (200 to 700 km), whereas others took into account the altitude range from 120 to 1200 km. Nisbet[10] constructed the first computer-based simple physical model MK-I for the ionosphere. He considered only three neutral constituents N_2, O_2 and O, whereas Stubbe[8] and Oran and Young[12] also considered the minor constituents He and H. For the dissociation and ionization of the neutral species, the incident solar EUV radiation in the range 30 to 1912 Å is used, along with the wavelength dependent absorption and ionization cross sections for the neutral species. Nisbet[10] considered three basic predominant ionic species: O^+, NO^+, and O_2^+. Oran and Young[12] took into account the additional ionic species N_2^+, He^+, N^+, and H^+. One has to consider the chemical reactions which produce ions by charge exchange processes. Nisbet[10] used 5 reactions whereas Oran and Young[12] used 24 chemical reactions (see Ref. 9). For maintenance of the ionosphere the processes of diffusion and photo-ionization are assumed. The processes of dissociative recombination and radiative recombination are responsible for the decay of the ionosphere. For his simple model, Nisbet neglected the transport processes such as neutral winds, electric fields, and magnetic fields. The procedure is further complicated because coupled simultaneous equations must be solved for neutral winds, mass transport, and energy transport. For determining electron density in the ionosphere, the gas, consisting of both ions and electrons, is considered electrically neutral. Thus, in every elementary volume, the number of electrons is equal to the number of ions. All the models reproduce many of the observed features such as the diurnal variation, seasonal variation, and solar cycle dependence of the mid-latitude ionosphere under quiet conditions. The accuracy of the theoretical models depends upon the understanding of the physical processes considered in the models. For accurate predictions from the theoretical models, precise information on the large number of variables used in the models is necessary.

Table 1. Variations in the Physical Processes Used in the Theoretical Models

Processes	Nisbet[10]	Stubbe[8]	Strobel and McElroy[9]	Oran and Young[11]
In the Altitude Region (km)	120-1250	120-1500	200-700	120-1200
Neutral Constituents for Ionization	N_2, O_2, O	N_2, O_2, O, He, H	N_2, O_2, O, He	N_2, O_2, O, He, H
Chemical Reactions (Charge-Exchange)	5 Reactions	10 Reactions	4 Reactions	24 Reactions
Ionized Constituents	O^+, NO^+, O_2^+	O^+, NO^+, O_2^+, [illegible]	O^+	O^+, NO^+, O_2^+, H^+ N^+, Ne^+, N_2^+
Neutral Winds	–	Horizontal Winds	Horizontal Winds	Horizontal Winds
Electric Fields	–	Yes	–	–
Magnetic Fields	–	Yes	–	–
Additional Features	–	–	–	Solar Flare Effects

Also, the models use several observed average boundary conditions which could have a large variability dependent on other geophysical parameters such as solar activity and magnetic activity. The results from the models are adequate for long term planning of science and engineering applications. Though these models reproduce main observed average features of the ionosphere, these are unable to specify the ionosphere within an accuracy of ± 20 percent needed by the systems in operation. At present, the main input information of solar EUV radiation needed for the theoretical models is not routinely available for predicting the ionosphere.

4. COMPARISON OF THE PHENOMENOLOGICAL MODELS, THEIR LIMITATIONS AND AVAILABILITY

In comparing the models one must note that 'IONCAP' is the modified and more flexible version which replaces the ITS-78 model. As the ITS-78/IONCAP and the Bent models serve entirely different purposes, it is essential to understand the difference in their approaches and final output parameters computed by the models. These are summarized in Table 2. The left-hand column in Table 2 lists the parameter under consideration. The next three columns summarize the features in each of the models, ITS-78, IONCAP, and the Bent model respectively. From the table it is seen that the selection of a model will depend more upon the information sought under the parameter headings than on accuracy. The IONCAP model is basically useful for wave propagation using operating frequencies which would be reflected by the E, E_s, F_1, and F_2 layers. On the other hand, the Bent model relies on the transmission, refraction, and absorption characteristics of the ionosphere, with the operating frequency much larger than the foF_2 frequency. All the models predict quiet ionospheric conditions only. The models do not hold for disturbed ionospheric conditions.

The additional limitations of these models are:

(1) All the models are poor in predicting the high latitude ionosphere,

(2) None of the models take into account the effects of particle precipitation in the auroral region which enhance the E (E_s) and F layers,

(3) The mid-latitude trough which exhibits large horizontal gradients in electron density is not incorporated in these models,

(4) These models are good for latitudes ± 20 to ± 60°, and are poor predictors for the equatorial region and the high latitude region.

Nonetheless these models serve two useful functions: (1) to predict ionospheric parameters; and (2) to determine physical phenomena and/or to modify existing coefficients for explaining the deviations between the experimentally observed value and the predictions from these models.

The computer programs for the ITS-78[1] and the IONCAP program[16] are available from the Institute for Telecommunications Sciences, Boulder Colorado 80303. The computer programs for the Bent model[14] are available from the Atlantic Science Corporation, P.O. Box 3201, Indialantic, Florida 32903.

Table 2. Intercomparison of the Empirical-Computer Based Ionospheric Models

Parameter	Ionospheric Models		
	ITS-78	IONCAP	Bent
D-Region	Non-deviative and deviative absorptions only	Same as ITS-78 + E Layer exponential extension down to 70 km	Not modeled
E-Region			
foE	Modeled by Leftin et al[22]	Same as ITS-78, + exponential down to 70 km. Leftin[17] coefficients	Not modeled
h_mE	110 km Fixed		
Y_mE	20 km Parabolic Shape		
F_1-Region	Not modeled		
foF_1		Rosich & Jones coefficients[18]	
h_mF_1 Y_mF_1		$h_mF_1/y_mF_1 = 4$ (fixed)	Not modeled
F_2-Region Bottomside			
foF_2	Hayden Lucas coefficients[23] Shimazaki eq, + E layer retardation Kelso[24]	Same as ITS-78	Bi-parabolic Bent coefficients.
h_mF_2			
Y_mF_2			
F_2-Region Topside	Not modeled	Not modeled	Up to 1000 km

(Due to large number of references cited in Table 2, they will not be listed here. See References, page 25.)

Table 2. Intercomparison of the Empirical-Computer Based Ionospheric Models (Cont)

Parameter	Ionospheric Models		
	ITS-78	IONCAP	Bent
E-F Transition Region	Not modeled	Modeled	Not Modeled
Electron-Density Profile	Not computed	Available up to $h_m F_2$	Available up to 3500 km
Total Electron Content (TEC)	Not computed	Not computed	Computed
MUF	For short path only	Also for long path (> 10,000 km)	Not modeled
Short-Term Prediction of MUF	Function of Kp	Not modeled	Not modeled
Input Parameters required	Sunspot number	Sunspot number	Sunspot number and 10.7 cm solar flux
Noise parameters	Galactic	Same	Not modeled
	Atmospheric	Modified	
	Manmade	Same	
MUF 50% FOT 90% $F_u = \frac{FOT}{MUF}$ HPF 10% $F_l = \frac{HPF}{MUF}$	Modeled	Modeled	Not modeled
System Performance	Modeled for short path (< 3000 km)	Also has a long path option ≥ 10,000 km	Not modeled
Antenna Patterns	Uses ITSA-1 Package with 10 antenna options	Modified ITS-78 package with 17 antenna options	Not modeled
Sporadic E	Modeled in terms of occurrence frequency	Same as ITS-78	Not modeled
Circuit Reliability Service Probability Multipath Evaluation	Modeled	Modeled as ITS-78	Not modeled

References

1. Barghausen, A.L., Finney, J.W., Proctor, L.L., and Schultz, L.D. (1969) Predicting Longterm Operational Parameters of High-frequency Sky-wave Telecommunication Systems, ESSA Tech. Report, ERL 110-ITS 78.
2. Bent, R.B., Llewellyn, S.K., and Walloch, M.K. (1972) Description and Evaluation of the Bent Ionospheric Model, Vol. I, SAMSO-TR-72-239.
3. Ching, B.K., and Chiu, Y.T. (1973) A phenomenological model of global ionospheric electron density in the E-, F_1-, and F_2- regions, J. Atmos. Terr. Phys. 35:1615.
4. Chiu, Y.T. (1975) An improved phenomenological model of ionospheric density, J. Atmos. Terr. Phys. 37:1563.
5. Kohnlein, W. (1978) Electron density models of the ionosphere, Rev. of Geophys. and Space Phys. 16:341.
6. Jones, W.B., Graham, R.P., and Leftin, M. (1966) Advances in Ionospheric Mapping by Numerical Methods, NBS Tech. Note 337, U.S. Govt. Printing Office, Washington, D.C.
7. Appleton, E.V., and Beynon, W.J.G. (1940) The application of ionospheric data to radio-communication problems: Part I., Proc. Phys. Soc. 52:518.
8. Stubbe, P. (1970) Simultaneous solution of the time dependent coupled continuity equations, and equations of motion for a system consisting of a neutral gas, an electron gas, and a four component ion gas, J. Atmos. Terr. Phys. 32:865.
9. Strobel, D.F., and McElroy, M.B. (1970) The F_2 layer at middle latitudes, Planet. Space Sci. 18:1181.
10. Nisbet, J.S. (1971) On the construction and use of a simple ionospheric model, Radio Science, 6:437.
11. Oran, E.S., Young, T.R., Anderson, D.V., Coffey, T.P., Kepple, P.C., Ali, A.W., and Strobel, D.F. (1974) A Numerical Model of the Mid-latitude Ionosphere, Naval Research Laboratory, Memorandum Report No. 2839.

PRECEDING PAGE BLANK-NOT FILMED

12. Oran, E.S., and Young, T.R. (1977) Numerical modeling of ionospheric chemistry and transport processes, J. Phys. Chem. 81:2463.

13. Jones, W.B., and Gallet, R.M. (1960) Ionospheric mapping by numerical methods, TTU Telecomm. J. 12:260.

14. Llewellyn, S.K., and Bent, R.B. (1973) Documentation and Description of the Bent Ionospheric Model, AFCRL-TR-73-0657, AD 772733.

15. Shimazaki, T. (1955) World wide variations in the height of the maximum electron density of the ionospheric F_2 layer, J. Radio Res. Labs., Japan 2:86.

16. Lloyd, J.L., Haydon, G.W., Lucas, D.L., and Teters, L.R. (1978) Estimating the Performance of Telecommunication Systems Using the Ionospheric Transmission Channel, National Telecommunications and Information Administration, Boulder, Colorado.

17. Leftin, M. (1976) Numerical Representation of Monthly Median Critical Frequencies of the Regular E Region (F_0E), OT Report 76-88, Boulder, Colorado.

18. Rosich, R.K., and Jones, W.B. (1973) The Numerical Representation of the Critical Frequency of the F_1 Region of the Ionosphere, OT Report 73-22, Boulder, Colorado.

19. Bradley, P.A., and Dudeney, J.R. (1973) A simple model of the vertical distribution of electron concentration in the ionosphere, J. Atmos. Terr. Phys. 35:2131.

20. Bradley, P.A., and Bedford, C. (1976) Prediction of HF circuit availability, Electronics Letters 12:32.

21. Flattery, T.W., Tascione, T.F., Secan, J.A., and Taylor, Jr., J.W. A Four-Dimensional Ionospheric Model (private communication).

22. Leftin, M., Ostrow, S.M., and Preston, C. (1968) Numerical Maps of foE_s for Solar Cycle Minimum and Maximum, ESSA Technical Report ERL 73-ITS-63, Boulder, Colorado.

23. Haydon, G.W., and Lucas, D.L. (1968) Predicting ionosphere electron density profiles, Radio Science 3:111.

24. Kelso, J.M. (1964) Radio Propagation in the Ionosphere, McGraw Hill, New York, N.Y.

GLOSSARY

a_k	Weighting factor in expression for electron density as a function of height.
a	Loss coefficient in the Chapman electron density profile.
foE	E-layer critical frequency.
foF_1	F_1-layer critical frequency.
foF_2	F_2-layer critical frequency.
foE_s	Sporadic E-layer critical frequency.
f	Operating frequency of communications system.
F_ℓ	Lower decile of f/f_m.
f_m	Median value of Maximum Usable Frequency.
F_u	Upper decile of f/f_m.
FOT	Optimum frequency for transmission.
h	Height.
h_s	Scale height of layer.
h_{max}	Height of maximum electron density.
h_mE	Height of maximum electron density within the E-layer.
h_mF_1	Height of maximum F_1-layer electron density.
h_mF_2	Height of maximum F_2-layer electron density.
k_1, k_2, k_3	Exponential constants in the Bent model for the three portions of the electron density profile above foF_2.
LUF	Lowest usable frequency.
MUF	Maximum usable frequency.
$N_e(h)$	Electron density as a function of height.
N_{emax}	Maximum electron density.
N_mE	Peak E-layer electron density.
N_mF	Peak F-layer electron density.
$W_k(\ell)$	Set of empirically derived discrete orthogonal functions for the altitude interval ℓ in the AFGWC 4-D model.
Y_mE	Half thickness of the E layer.
Y_mF_1	Half thickness of the F_1 layer.
Y_mF_2, Y_t	Half thickness of the F_2 layer.


DATE
FILME
7 — 8